51. Measurement Systems for Wind, Solar and Hydro Power Applications

Stefan Emeis , **Stefan Wilbert**

Wind, solar, and hydropower are major forms of the so-called renewable energies. Effective application of renewable energies to supply heat and electricity is weather dependent and needs short-term weather forecasts, as well as historical and climatological information. All relevant measurement sensors were introduced in previous chapters. Here, the special requirements of wind, radiation, and precipitation measurements for planning and operating renewable energy power plants are addressed. The cooling of conventional thermal power plants, the transmission of electricity in cables above ground, and the overall energy demand are weather dependent as well, and thus need atmospheric measurements.

Meteorological competence directed to a meaningful and smooth application of devices that supply electricity and heat from fossil and renewable energy sources is summarized in the subdiscipline "energy meteorology" today. Energy meteorology comprises theoretical considerations, data capture, data analysis, and weather forecasts relevant to power generation, distribution, and consumption. Energy meteorology for wind energy is covered in [51.1]. For solar energy applications, more detailed information is provided, e.g., in [51.2]. For hy-

dropower applications, the reader can refer to [51.3] for more details. A short review on the present status of the whole subject is found in [51.4].

Although fossil and renewable energy supply devices have been operated for a long time, energy meteorology mainly developed during the last three decades due to the growth of the renewable energy capacity and its much larger need for meteorological information compared to fossil power plants. With a few exceptions the main difference in the required meteorological

knowledge for power generation purposes is that for fully fossil power plants, meteorological information is mainly needed in order to assess the load (e.g., high loads during cold spells). For renewable energy, meteorological information is also needed to estimate the energy production.

51.1 Measured Parameters

Table 51.1 gives an overview on the meteorological parameters needed for the planning and operation of renewable energy sources and an electricity grid with fossil and renewable energy sources. The parameters are listed next to the form in which the parameter is required, its application, unit, and symbol.

The deployment of measurement instruments for site assessment or performance monitoring of renewable energy power plants will be very much determined by the intended use of the generated power (e.g., the instantaneous generation of electricity or the accumulative storage of heat). The main requirement is that the measurements are representative for an area or an air volume covered by the foreseen devices for power generation. For instance, wind measurements often have to be performed at exposed sites, such as hilltops. In this case, attention has to be paid to the problem of curved streamlines, as described in Sect. 23.6.3 of this

Table 51.1 Measured parameters used in renewable energy applications

Parameter	Form	Relevance	Unit	Symbol
Wind speed	Time series, statistics, extreme values, vertical profiles	Wind energy, power lines, solar energy	$\mathrm{m\,s^{-1}}$	u
Wind direction	Time series, statistics, vertical profiles	Wind energy, solar energy	°	
Air temperature	Instantaneous values (wind energy, power lines, cooling towers), weekly or monthly average (cooling water for hydropower)	Wind energy (air density, risk of icing), power lines, solar energy, hydropower (evaporation, warming of cooling water), operation of cooling towers, load estimations	K	T
Pressure	Time series, statistics	Wind energy (air density), power lines, cooling towers	hPa	p
Humidity	Instantaneous values, weekly or monthly averages	Wind energy (air density, risk of icing), hydropower (evaporation), operation of cooling towers, power lines	% (relative humidity), $10^{-3}\,\mathrm{kg\,kg^{-1}}$ (absolute humidity)	RH, q
Global horizontal irradiance	Time series, statistics, extreme values	Solar energy, hydropower (evaporation), power lines	$\mathrm{W\,m^{-2}}$	G (according to [51.5]), often GHI, atmospheric sciences use $K\downarrow$
Direct normal irradiance	Time series, statistics, extreme values	Concentrating solar technologies	$\mathrm{W\,m^{-2}}$	G_b, according to [51.5], also DNI
Global tilted irradiance	Time series, statistics, extreme values	Non or low concentrating photovoltaic plants, flat plate collectors	$\mathrm{W\,m^{-2}}$	G_t, also GTI
Beam attenuation	Time series, statistics	Solar tower plants	–	A
Solar and circumsolar radiance profile	Time series, statistics	Concentrating solar technologies	$\mathrm{W\,m^{-2}\,sr^{-1}}$	S
Circumsolar contribution	Time series, statistics	Concentrating solar technologies	–	CSC
Soiling rate	Time series, statistics, extreme values	Solar energy	$\mathrm{s^{-1}}$	$\hat{\xi}$
Solar spectral irradiance	Time series, statistics	Photovoltaic plants	$\mathrm{W\,m^{-2}\,\mu m^{-1}}$	E_λ
Precipitation	Amount and intensity (spatial averages), time series, statistics, extreme values, form (snow, hail)	Hydropower, solar energy	L, mm	P
Snow cover	Amount	Solar energy	cm	

book, which is relevant for remote sensing of wind profiles in complex terrain. Normal representativeness considerations, which are relevant for climatological and meteorological studies, and which have been listed in the respective sections of this handbook, cannot be fulfilled in every case. Therefore, further hints and details for power-related measurements can be found in Sect. 51.4.

51.2 History

The usage of renewable energies and the operation of classical fossil energy infrastructures (power plants and power lines) are based on existing meteorological expertise and data and site-specific measurements (see the sections below). By around the turn of the millennium the paramount importance of meteorological data for the operation of renewable energies became clearer, and the subdiscipline energy meteorology started to emerge. The first German specialty conference on energy meteorology took place 2009. The inaugural International Conference on Energy & Meteorology was convened in Australia in 2011. The development of renewable energies is very much driven by private companies. Thus, additional site-specific measurements up to now have very often been planned and executed by these private companies. This data is usually not publicly available.

51.2.1 History of Measurements for Wind Energy

Wind measurements have accompanied the usage of the kinetic energy contained in winds through all times. Traditional windmills have been built for centuries in Europe, and the growing political and economic importance of sailing ships in the eighteenth and nineteenth centuries led, e.g., to the development of the Beaufort wind scale. Compared to this the construction and deployment of wind turbines for the generation of electricity was a rather new development that emerged in the twentieth century. In the beginning until the 1980s, 10 m wind data were extrapolated to the then hub heights of the first wind turbines of less than 50 m. Later, the erection of meteorological masts became the most accepted wind assessment technology, when hub heights were about 50 m and above. In the 1990s, the interest in surface-based acoustic remote sensing (Chap. 23) grew, since the deployment of taller masts in the order of 100 m height became more expensive than ground-based acoustic remote sensing, although the trust in remote-sensing data remained less than the trust in in-situ cup anemometer measurements. A major reason for the persisting trust in cup anemometer data was that these instruments could be easily calibrated in wind tunnels.

In the 2000s, optical remote sensing (Chap. 27 on wind lidars) took over from sodars, because wind lidars became commercially available, and the data availability of wind lidars is considerably better than that from sodars. After 2015, wind energy guidelines [51.6] started to accept optical remote sensing as an independent source for reliable wind data.

Specific data capture for the development of offshore wind farms started with large masts as well. Near-coastal masts were, e.g., erected close to the Danish west coast at a wind turbine test site at Høvsøre in 2002 [51.7]. In the German part of the North Sea, the first real offshore meteorological mast about 45 km off the coast was erected (the 100 m-high mast FINO 1 [51.8]) in 2003. Two more similarly instrumented masts (FINO 2 in the Baltic Sea and FINO 3 in the northern part of the North Sea) followed a few years later. Remote sensing was no option for these offshore measurement platforms, because acoustic remote sensing due to unavoidable fixed echoes (Chap. 23 on sodars and RASS) was not possible close to the mandatory masts on these platforms, and optical remote sensing was not commercially available at the time of planning the first of these measurement platforms. Even today, wind lidars are not part of the standard instrumentation on these three platforms. Such devices were only brought to the platforms during limited measurement campaigns.

Specific data for winds in complex terrain are available from a 200 m-mast erected on the Rödeser Berg near Kassel, Germany, at the end of 2011 [51.9]. A test site for wind turbines in complex terrain exists south of Boulder, Colorado, close to the foothills of the Rocky Mountains [51.10]. A further wind turbine test site with meteorological masts close to an about 200 m-high escarpment is presently being designed and erected east of Stuttgart, Germany.

Temperature profile measurements to assess the thermal stratification of the atmospheric boundary layer for the purpose of generating energy from the wind are rarely executed. For a long time, the impact of thermal stratification on wind energy generation was considered to be negligible with higher wind speeds. Today, for issues such as low-level jets and wake propagation, these measurements appear to be more and more necessary for a proper assessment of wind energy.

51.2.2 History of Measurements for Solar Energy

Solar energy applications have a long history, starting centuries before the first solar radiation measurements became possible (Chap. 11 for the history of radiation measurements). The first simple solar heating and lighting applications did not require the measurement of solar radiation or other meteorological parameters. By the end of the nineteenth century *Augustin Mouchot* (1825–1911) developed the first solar powered engine [51.11], which was demonstrated at the Universal Exhibition in Paris in 1878. At the latest then atmospheric data were required for solar energy in order to decide whether or not this new technology was a competitive alternative to other power sources, such as coal. Apparently, decision-makers estimated that this was not the case, as more intense research on solar energy started only after World War II. By then, pyrheliometers and pyranometers were already available, as well as measurement systems for most of the other relevant atmospheric parameters. These instruments could be used for performance testing and system characterization, two main applications of meteorological measurements for solar energy. With the growing interest in solar energy in the 1970s due to the oil crisis, it became increasingly clear that the already available meteorological data were not enough to provide a good estimate of the solar resource available at a given site and, hence, the corresponding expected power plant yield. Due to the spatial variability of meteorological conditions and, in particular, solar irradiance it was found that the resource data must be collected for a site close to the envisioned power plant site. Even today data from ground-based measurements are not available close to most potential power plant sites. Therefore, existing measurement networks were enhanced and model approaches were investigated.

As interesting power plant sites are often remote, it is often not feasible to maintain pyranometers and pyrheliometers good enough to achieve the desired accuracy. Therefore, and to reduce the costs of the instrumentation, less maintenance intense instruments, such as the rotating shadowband irradiometer (RSI) were developed [51.12]. Such instruments were continuously improved and are widely used for solar energy applications, especially for the planning of solar power plants.

Even if a measurement station is deployed for the resource assessment at a site, the dataset is typically too short to analyze the interannual variability of the irradiance well enough for the determination of the expected solar plant yield. Therefore, methods to derive long-term datasets were developed. Long-term datasets are mostly derived from related measurements. His-torically, modeling efforts included the determination of global horizontal and direct normal irradiance from sunshine duration measurements [51.13], as these were much more frequent than pyranometric or pyrheliometric measurements. Today, irradiance models based on sunshine duration are only of historic interest and are no longer recommended according to best practices [51.2]. Modeling efforts also included the creation of irradiance maps, for example based on interpolation techniques between the stations. Such spatial interpolations are still used today in some cases, but the application of satellite derived long-term datasets is much more common. Satellite-based measurements of the radiation reflected from the ground or clouds to the satellite have been used to derive irradiance since the 1980s (Chap. 40) and have become a standard data source for the planning of solar power plants.

Today, combinations of satellite and ground-based measurements are used for the planning of large solar power plants with several MW output power, as will be explained in more detail in Sect. 51.4.5. Due to the growing grid penetration of solar energy irradiance forecasting systems were developed in the last two decades. These systems also rely on ground measurements of irradiance, ground-based all-sky imagers and/or satellite data.

51.2.3 History of Measurements for Hydropower

Since there has not been much development in the usage of hydropower in the last decades, the means of measurements have not changed either. Hydropower relied and still relies on monitoring the discharge of rivers for hydropower plants at rivers and the water level in natural and artificial reservoirs for hydropower plants operating below such reservoirs.

51.2.4 History of Measurements for Conventional Power Plants, Grid Operation, and Electricity Transmission

Engineering sciences have dealt with the weather impact on conventional power plants, electricity transmission structures, and grid operations. Meteorological data was required for these assessments, but no special measurement techniques have been developed for this purpose.

Measures such as heating degree days (HDD) [51.14] and cooling degree days (CDD) [51.15] have been developed for the assessment of the energy demand. However, these measures were computed from the available classical weather and climate data.

51.3 Theory

This section summarizes the relevance of the different atmospheric parameters for the different forms of power generation (see the respective column in Table 51.1). A proper operation of power grids (and less strictly, also heating/cooling systems) requires a nearly perfect balance of generation and consumption at any moment. Therefore, atmospheric parameters are necessary to assess the production potential, as well as the expected consumption. These estimates have to be supplied at least 1 day ahead and then have to be refined in several steps until 15 min before the very moment. For example, the regulation of the electricity grid in Germany is performed by trade at the energy stock exchange in Leipzig. Expectations computed from atmospheric data are the basis for this trade. The generation of electrical energy from wind power depends on meteorological parameters in several respects, which are addressed in the following.

51.3.1 Dependence of Wind Energy on Meteorological Parameters

The harvest of electrical energy from the wind principally depends on the third power of the wind speed [51.1], as long as the rated power of the used wind turbines is not reached. Between the rated power of the turbines and the cut-off wind speed (see below) the harvested electrical energy is maximum and independent on wind speed. Additionally, the energy harvest below the rated power of the turbines depends on air density. Cooler and dryer air is denser than warmer and more humid air. The energy harvest is linearly proportional to the density of the air.

The power available from the wind energy, P_{wind} in atmospheric flow, i.e., the kinetic energy of the air, $0.5\rho u^2$ advected with the wind, u is quantified by the following relation

$$P_{\text{wind}} = 0.5\rho A_{\text{r}} u^2 u = 0.5\rho A_{\text{r}} u^3 , \tag{51.1}$$

where ρ is the air density, A_{r} is the rotor area of the turbine, and u is the average wind speed over the rotor area. Equation (51.1) gives the available wind power over the rotor disk in Watt when the air density is given in kg m^{-3}, the rotor area in m^2, and the wind speed in m s^{-1}. Theoretically, turbines can extract up to $16/27$ of this power [51.16, 17]. This limit is known as Betz limit today.

Assessments of annual energy harvest potentials not only depend on the mean annual wind speed but also on the distribution of the wind speed due to the nonlinear dependence of the energy harvest on the wind speed. Weibull (Swedish engineer, scientist, and mathematician *Ernst Hjalmar Waloddi Weibull*, 1887–1979) statistics [51.18] are usually computed for the annual distribution of 10 min mean wind speeds. Additionally, Gumbel (German mathematician *Emil Julius Gumbel*, 1891–1966) statistics [51.19] are used to estimate extreme 10 min mean wind and gust speeds that are load relevant. The probability $F(u)$ of the occurrence of a wind speed smaller or equal to a given speed u is expressed in terms of the Weibull distribution by

$$F(u) = 1 - \exp\left(-\left(\frac{u}{A}\right)^k\right), \tag{51.2}$$

where A is the scale factor of this distribution in m/s, and k is the shape factor. Once the two factors A and k are known, the available annual wind power resource can be computed by replacing u^3 in (51.1) by the third central moment of the Weibull distribution

$$E_{\text{wind}} = 0.5\rho A_{\text{r}} A^3 \Gamma\left(1 + \frac{3}{k}\right), \tag{51.3}$$

where Γ is the Gamma function.

The Gumbel distribution gives the probability $F(u)$ of the occurrence of a wind speed smaller than or equal to a given speed u by

$$F(u) = e^{-e^{-(u-a)/b}} , \tag{51.4}$$

with the scale factor a and the shape factor b (both in m/s). An extreme value is then computed from known factors a and b by

$$u_{\text{max}} = a(-\ln(-\ln(p))) + b , \tag{51.5}$$

where the probability p depends on the number of available data within the addressed return period. The probability of a, e.g., 50-year extreme from such a time series with 10 min-intervals (52 560 data points a year) is given by $p = 1 - 1/(50 \times 52\,560)$, giving $-\ln(-\ln(p)) = 14.78$. For a time series with hourly values, the threshold value would be 12.99.

Wind turbines only run when the 10 min mean wind speed is in a certain range of wind speeds. They start to operate at the cut-in wind speed of $4-5$ m/s. They usually stop operating at the cut-off wind speed of 25 m/s. The cut-off at higher wind speeds is necessary in order to avoid too large loads on the wind turbines.

The vertical profile of wind speed is of paramount importance for wind energy. For the assessment of energy yields and mean loads on today's large rotors

with diameters of much more than $100\,\mathrm{m}$, the rotor-equivalent wind speed (REWS) is computed from an (rough) integration of the wind speed distribution across the rotor plane. The provision of wind speed profiles with a vertical resolution of about $20-30\,\mathrm{m}$ is necessary for the computation of rotor-equivalent wind speeds. The 2017 version of the IEC standard 61400-12-1 [51.6] now refers to the REWS, which is defined by a weighted sum of the cubes of simultaneous wind speed measurements at a number of heights spanning the complete rotor diameter between lower tip and upper tip [51.20]

$$v_{\mathrm{eq}} = \left(\sum_{i=1}^{n} v_i^3 \frac{A_i}{A} \right)^{1/3} \quad \text{with} \quad \sum_{i=1}^{n} A_i = A , \quad (51.6)$$

where n is the number of measurements across the rotor area, v_i is the 10 min mean wind speed at height $z = z_i$, A_i is the area of the i-th rotor segment, and A is the total rotor area. The segment areas are computed between two lines z_j and z_{j+1}, which are positioned exactly halfway between two measurements

$$A_i = \int_{z_j}^{z_{j+1}} c(z)\,\mathrm{d}z , \quad (51.7)$$

where $c(z)$ is the area of a segment of a circle

$$c(z) = 2\sqrt{R^2 - (z-H)^2} , \quad (51.8)$$

where R is the rotor radius, and H is the hub height.

Loads on wind turbines increase with increasing vertical shear and increasing turbulence intensity. The turbulence intensity is given by

$$I_u(z) = \left(\ln\left(\frac{z}{z_0}\right) - \Psi_m\left(\frac{z}{L_*}\right) \right)^{-1} . \quad (51.9)$$

This means that turbulence intensity increases with shear (the left-hand term of (51.9)) and with decreasing stability (the right-hand term of (51.9)); Ψ is the integral correction function for atmospheric thermal stability [51.21–25]. See Chap. 1 for a basic treatment of this parameter. Several extreme atmospheric phenomena such as gusts, thunderstorms, lightning, and icing have an impact on the operation of wind turbines.

51.3.2 Dependence of Solar Energy on Meteorological Parameters

Here, we have to differentiate between different available solar energy technologies (Fig. 51.1). Common photovoltaic (PV) plants and nonconcentrating solar heating and cooling collectors use the global tilted irradiance (G_{tilt}) incident on the collector plane. Bifacial

PV modules also use the in-plane rear-side irradiance. PV modules can also be tracked in one or two axes to increase G_{tilt}; PV cells can also be mounted behind a focusing lens or in the focal point of mirrors that are tracked to the sun. In this case, direct normal irradiance (G_{b}) is used. This is also the case for concentrating solar power (CSP) plants that use mirrors to focus the direct radiation on an absorber to create heat. This heat can be used for industrial processes, heating, cooling, or to generate electricity using a thermodynamic cycle. Depending on the plant type, actually not G_{b}, but its projection on the collectors' aperture is used. This projection is calculated in plant models, and G_{b} is provided as a result of the meteorological measurements. Low concentrating PV collectors are tracked to the sun and only have a small ratio of the aperture to the PV cell surface. In this case, G_{b} and another diffuse fraction of G_{tilt} is used. The fact that different technologies use different components of solar radiation greatly affects their production. Clouds and fog diminish the yield of all solar collectors, but concentrating collectors are much more sensitive to clouds and fog than flat-plate collectors and nonconcentrating PV, as they only use direct radiation.

The specification of direct normal irradiance (G_{b}) is actually not a complete description of the resource used for concentrating collectors. Depending on the concentrator and the receiving surface, radiation from a different angular region around the sun is used by solar collectors. While pyrheliometers measure the irradiance coming from an approximately $2.5°$-wide circular region around the sun (half-angle), most concentrating solar plants for solar thermal electricity generation and high concentrating PV systems accept only a narrower region (e.g., $1.5°$). For concentrating PV systems and process heat collectors, also wider acceptance angles can be found. This effect is accounted for in state-of-the-art plant models, but this requires another input parameter – the sunshape. The sunshape is the radiance of the sun and the circumsolar region closely around the sun as a function of the angular distance from the center of the sun, normalized to 1 in the center of the sun. The description of the radiance distribution with a sunshape corresponds to the assumption that it is radially symmetric. The sunshape can be characterized by the circumsolar contribution: the ratio of the circumsolar normal irradiance coming from a given angular region between an inner and an outer boundary angle close to the sun and the direct normal irradiance including radiation from the solar disk and the circumsolar radiation up to the outer boundary angle.

For flat plate collectors and nonconcentrating PV, also the angular distribution of the irradiance is of interest, as the efficiency of the collectors depends on the incidence angle. The specification of the contribution

Fig. 51.1a–d Solar collectors at CIEMAT's Plataforma Solar de Almería. (**a**) Tower plant CESA-1, (**b**) parabolic trough collector, (**c**) solar thermal collector, and (**d**) photovoltaic plant ((**a**) photo © Christoph Prahl, DLR, (**b–d**) photos © Stefan Wilbert, DLR)

of direct and diffuse irradiance to G_{tilt} is nearly always sufficient for such models.

In the case of PV, also the spectral distribution of the irradiance is of importance, as PV cells only use a certain part of the solar spectrum. Furthermore, the efficiency of PV cells varies strongly on the incoming wavelength, even within the accepted wavelength interval.

Besides radiation several other parameters affect the solar plant yield. PV cells operate most efficiently at low module temperatures. Thus, air temperature and wind speed are relevant as well. Thermal collectors operate more efficiently in warm conditions with low wind speeds, as heat losses are lower in such cases. However, the cooling for the thermodynamic cycle of CSP plants is less efficient for high temperatures and low wind speed. Also the pressure and humidity affect cooling.

Wind speed, direction, and wind gust also pay another important role in solar power generation, as wind can damage the plant components. This is of high importance for tracking collectors that do not withstand strong winds in operation, but only in a security position (stow position). This leads to production losses, as the collectors might not be able to collect energy (CSP, high concentrating PV), or as they will only collect significantly less radiation (tracked PV systems, low concentrating PV).

The effects of precipitation are descriptive. Snow cover on the collectors stops their operation while snow infront of a snow free PV module or flat plate collector increases the ground reflected radiation on the collector. Very large hail stones are a threat to the integrity of solar collectors. Rain accumulating on the collector surface reduces its transmittance or reflectance, but it can also have positive effects. One positive effect is the cooling of the PV module. Another positive and more relevant effect is the potential cleaning of the collectors. Atmospheric dust can settle on the collectors and greatly reduce the transmittance or reflectance. This effect is described by the cleanliness, which is the ratio of the efficiency in the current potentially soiled status of the device and the efficiency of a clean device under otherwise unchanged conditions. Soiling is described by the soiling rate, the change of the cleanliness with time. Note that at times, rain actually does not clean the collectors but on the contrary decreases the cleanliness by wet deposition of particles.

For solar tower plants, another parameter is of high relevance: the atmospheric extinction between the mirrors (heliostats) and the receiver. The path between the heliostats and the receiver can be greater than 1 km. Even for a clean, dry atmosphere with a high visibility of about 75 km, about 5% of the reflected radiation is lost on a 1 km light path to the receiver. For hazy conditions, this loss can be 100%, and high losses of about 50% can occur even at high direct irradiance levels.

51.3.3 Dependence of Hydropower on Meteorological Parameters

Assessment of hydropower potentials requires the capture of areal instantaneous and seasonal averaged precipitation amounts in the catchment areas of rivers and reservoirs. Evaporation processes are only relevant, if the water is to be stored over several months or even years. See Chap. 57 for evaporation measurements and calculations.

Peak river discharges depend on the precipitation amounts of the last hours and days in the catchment area of rivers. Soils saturated with moisture from preceding precipitation events enhance the river discharge, because most of the new rain water cannot infiltrate the wetted soil and runs off immediately. Thus, the soil's water content in the catchment area is to be monitored as well. In springtime, melting snow covers in the catchment area can contribute considerably to river discharges. Long frost periods, dry spells, and droughts can cause very low river discharges. The water levels in reservoirs depend on longer-term precipitation amounts over a few days to months. Again, melting snow and ice from the last winter can contribute considerably to the water level.

51.3.4 Dependence of Thermal (Conventional) Power Plants on Meteorological Parameters

Temperature and humidity influence the conditions for wet cooling towers and water cooling of thermal power plants. In a wet cooling tower (or open-circuit cooling tower), warm water can be cooled to a temperature lower than the ambient temperature. As ambient air is drawn past a flow of water, a small portion of the water evaporates, and the energy required to evaporate that portion of the water is taken from the remaining mass of water, thus reducing its temperature. This type of cooling is most effective when the saturation deficit of the air is large.

If sufficient water is available (at the banks of larger rivers) direct cooling using water from the river (once-through cooling) can be used. Here, the efficiency depends on the temperature of the water from the river. Often, the warming-up of the water from the river downstream of the power plant is limited by regulations to a given threshold temperature for ecological reasons. If the temperature of the water upstream of the power plant already exceeds this threshold temperature, once-through cooling is no longer permitted.

In longer drought situations, low water levels in rivers can cause problems in transporting the necessary coal to the power plants. In hard winters, the coal could also be frozen in goods waggons, which hampers the supply of power plants as well.

51.3.5 Dependence of Energy Transmission on Meteorological Parameters

Cables in overhead transmission lines warm up in operation proportionally to the electrical resistance of the

cable and the strength of the electrical current flowing through them. Warmer cables expand, and, thus, transmission cables hanging from masts sag more and come closer to the ground. In order to prevent excessive sagging, the temperature of these cables must be limited. Normal high-voltage transmission cables with steel cores are not allowed to warm up to more than $80\,°C$ during normal operation and $100\,°C$ at peak operation. Special ACCC (aluminum conductor composite core) cables have a smaller thermal expansion coefficient and can be operated up to a temperature of $175\,°C$.

On the other hand, the temperature of transmission cables is influenced by the environmental atmospheric conditions [51.26]. The cables are cooled by heat conduction to the air flowing past them, and they are warmed up by absorbing incoming short-wave radiation. The cooling depends on wind speed, air density, and the heat conductivity of the air. Air density and heat conductivity depend on air pressure, temperature, and humidity. Without any temperature monitoring transmission cables must be operated according to the worst-case scenarios given in standards and guidelines (e.g., [51.27]) assuming $35\,°C$ air temperature, $0.6\,\mathrm{m\,s^{-1}}$ wind speed, and $900\,\mathrm{W/m^2}$ global radiation. Monitoring the cable temperature and/or near-cable atmospheric data can help with a much more efficient use of the transmission cables.

The accretion of ice at transmission cables could become a problem in wintry weather situations, when rain falls from warmer layers above into colder near-surface air layers with temperatures below the freezing point. This may sometimes happen in the case of approaching warm fronts. The weight of the accreted ice can lead to extreme sagging of cables. In some cases, even the breaking of cables and entire electricity pylons has been observed. Excessive riming in the case of advection of very humid air masses and fog to power cables at temperatures below the freezing point can lead to similar effects.

Extreme winds may be a hazard for above-surface power lines and electric pylons as well. This could be the direct impact of the wind on the power lines, as well as the impact of falling trees and other structures on these lines.

51.3.6 Dependence of Energy Demand on Meteorological Parameters

Electric energy demand for heating and cooling, as well as lighting of living places and work spaces depends on the ambient air temperature, wind speed, incoming daytime short-wave radiation (especially direct normal irradiation), and nocturnal long-wave radiation. Very often, heating-degree days [51.14] and cooling-degree days [51.15] are used as an approximate measure to assess the demand for heating and cooling. It is anticipated that the future energy demand for individual electric mobility is temperature-dependent as well, because the performance of batteries is strongly temperature dependent.

51.4 Devices and Systems

Many of the devices and systems described in detail earlier in this handbook and briefly in [51.28] are used to capture the necessary data for running energy systems. This section summarizes specific comments on some of these devices. Precipitation gauges are described in Chap. 12.

51.4.1 Cup and Sonic Anemometers

Near-surface wind speed is very often measured by cup anemometers (Chap. 9) that have been calibrated in wind tunnels. Site-specific wind speed measurements up to heights in the order of $50-100\,\mathrm{m}$ are quite often made from masts erected for this purpose. See Chap. 9 on anemometry and [51.29] for details. Measurements of turbulence are described in [51.30]. Cup and sonic anemometers deliver scalar means of wind speed representative for small measurement volumes (in-situ measurements). Sonic anemometers are also able to deliver turbulence measurements. Because they are much more expensive than cup anemometers, sonic anemometers have not found widespread usage in wind energy so far, but their usage is increasing. For instance, they have now found a role in wind turbine nacelles for wind speed and yaw control purposes. Appropriate calibration standards comparable to those for cup anemometers have not yet been developed [51.31].

51.4.2 Surface-Based Remote Sensing of Wind and Temperature

Today's wind energy applications require knowledge of vertical wind distributions above those heights that can meaningfully be reached by mast measurements. Surface-based remote sensing has been used for this purpose for about 20 years [51.32]. The first sodars were deployed at potential wind energy sites, and now Doppler wind lidars are operated, because they promise

better data availability, a higher vertical range, and less environmental interference. See Chap. 23 and [51.33] for details on sodars and Chap. 27 and [51.34] for details on wind lidars. Wind profile measurements together with temperature profile measurements are available from radio-acoustic sounding systems (RASS) as well. RASS are described in Chap. 23 and [51.35]. Remote sensing of wind profiles would also be feasible with wind profilers (Chap. 31 and [51.36, 37]), but these instruments are not movable, and they do not have sufficient vertical resolution in the height range of wind turbines. Remote sensing delivers vector means of wind speed for larger measurement volumes determined by the pulse length and the opening angle between the beams originating from the instrument.

Passive radiometers (Chap. 29) are also designed to measure vertical temperature (and humidity) profiles. However, their vertical resolution is in the order of 50 and 100 m, which is not sufficient for wind energy purposes. Scanning at very low elevation angles in order to obtain a better vertical resolution would result, in turn, in more extended horizontal averaging, which in most cases is unwanted in energy site assessments.

51.4.3 Satellite Wind Observations

A meaningful option to capture areal distributions of offshore near-surface winds is the analysis of synthetic aperture radar (SAR) images from satellites. SAR data allow for a determination of the near surface wind speed and the detection of spatial gradients in these near-surface wind fields from the observation of capillary waves on the ocean's surface [51.38]. Capillary waves are supposed to change nearly immediately with the near-surface wind speed. These small-scale waves cause scattering of the radar waves emitted from the satellite, and less radiation is scattered directly backwards towards the satellite during the presence of these waves.

Principally, the evaluation of these images gives near-surface winds only. It is only the application of vertical extrapolations based on wind profile laws (i.e., the logarithmic law with possible corrections for atmospheric thermal stability or the power law with a suitable exponent) that allows the estimation and assessment of the hub height wind speed for wind energy applications. However, these extrapolations need additional input data, especially the vertical temperature profile. Nevertheless, the usability of SAR images to detect offshore wind-farm wakes was proven for the first time in [51.39]. First comparisons between SAR images and mesoscale wind simulations using the weather research and forecasting WRF model have been shown in [51.40]. The results from model simula-

tions and SAR images were proved for the first time by aircraft measurements behind North Sea wind farms in 2016 [51.41]. See Chap. 41 on microwave radiometers as well.

51.4.4 Measurement Stations for Solar Energy

During the planning, commissioning, and operation of large solar power plants with a capacity of about 1 MW or more on-site measured meteorological data are required. Meteorological measurements are also necessary for the testing of solar plant technologies.

Radiometers are the core of measurement stations for solar energy. Radiation measurements are described in Chap. 11. Also the other relevant and typically measured parameters have been discussed in previous chapters (wind speed and direction in Chap. 9, air temperature in Chap. 7, humidity in Chap. 8, pressure in Chap. 10, and precipitation in Chap. 12).

The instruments, their application and maintenance for solar energy applications are basically the same as for other atmospheric measurements. However, there are some differences. Specific recommendations for solar energy related measurements can be found in [51.2, 42]. The mentioned differences are caused basically by two reasons. First of all the measurements must characterize the conditions at the power plant site or in the plant. Therefore, stations must at times be positioned such that they do not fulfil fundamental requirements of measurements carried out for other purposes. For example, in the case of climate research, a free horizon is recommended for the site with no obstructions above 5° elevation [51.43]. For climate research, the baseline surface radiation network (BSRN) recommends that stations should not be close to major roadways or airports [51.44]. For the maintenance of the station during the solar resource assessment and for the costs of the power plant construction such infrastructure can be of great advantage, so that such recommendations do not apply to solar energy-specific measurements. Obviously, such differences also exist for other meteorological applications, such as transport meteorology, where measurements must be carried out close to airports and roads. The second reason why solar energy specific measurements might deviate from other atmospheric measurement stations is that different applications also bring along different optimal cost/benefit ratios. The most important example for this is that it is often not feasible to set up a high accuracy measurement station with a solar tracker and thermopile sensors (Fig. 51.2a) at the envisioned plant site for the resource assessment if this site is remote. For such sites, it is often impossible or at least too costly to assure
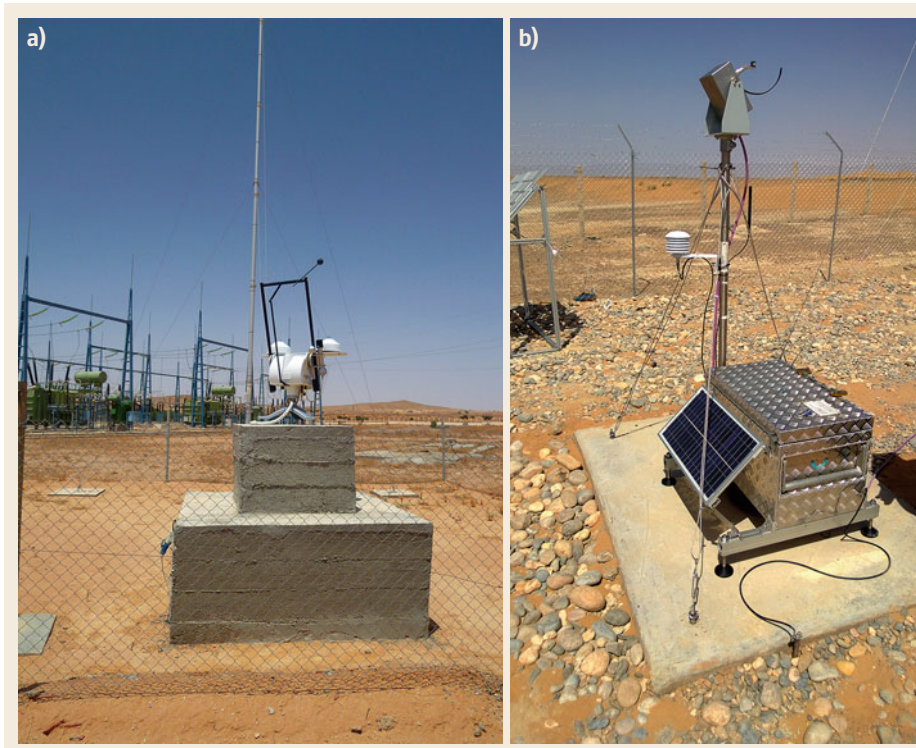
Fig. 51.2
(**a**) Measurement station for solar resource assessment in Tataouine, Tunisia, equipped with thermopile radiometers, cup anemometer, wind vane, pressure, temperature, and relative humidity sensors. (**b**) Rotating shadowband irradiometer as part of a solar resource assessment station close to Erfoud, Morocco (photos © Birk Kraas, CSP-Services)

the required daily maintenance by sufficiently qualified personnel. Reduced cleaning frequency and the corresponding soiling of the entrance windows is especially relevant for pyrheliometers, but also pyranometers with clear entrance windows suffer from soiling. Therefore, less maintenance intense sensors, such as rotating shadowband irradiometers (RSI, at times also called RSP or RSR, with P for pyranometer and R for radiometer) are often used at remote sites (Fig. 51.2b). They achieve lower accuracy in well-maintained stations with daily cleaning of the instruments' entrance windows, but if specific correction functions are applied, a better accuracy is reached for less frequent maintenance [51.45], for example only once every week or every 2 weeks. Correction functions are needed, as simple silicon pyranometers with higher incidence angle, temperature, and spectral errors are used in most cases. The lower maintenance requirement is due to the fact that RSIs apply pyranometers with diffusors in front of the detector, without an additional clear entrance window. Furthermore, RSIs are cheaper than thermopile sensors with solar trackers and are more robust and simpler, which leads to less frequent malfunctions, user mistakes, and data loss [51.46]. Another option to reduce the cost and maintenance requirements compared to pyrheliometers are instruments with sensor arrays and specific shading structures that avoid the requirement

of any moving part for direct irradiance measurements. However, unlike RSIs, such instruments still require the same cleaning frequency as thermopile pyranometers. An example of such a sensor is the SPN1 radiometer [51.47].

A significant cost reduction of a meteorological station can be achieved if direct normal irradiance (G_b) is not measured. For concentrating solar power plants (CSP and concentrating PV), G_b is required, and for tracked PV plants and large power plants it is desirable. For concentrating technologies, this is obvious. For the other plants mentioned, in principle, only global tilted irradiance G_{tilt} must be known. However, for more accurate plant yield calculations, the direct component in G_{tilt} is of interest, as mentioned in Sect. 51.3.2. In the case of tracked PV collectors, G_{tilt} measurements would also require a tracker for the pyranometer, so that no significant cost advantage remains. Furthermore, measuring the three radiation components (direct, global, and diffuse) allows for a better quality control of the data, which is of high value. For fixed collectors, G_{tilt} can be measured with an adequately mounted pyranometer without a solar tracker. Typically, for solar resource assessments for fixed PV and flat plate collectors, common global horizontal irradiance measurements are used combined with conversion models to derive G_{tilt}.

The sunshape and circumsolar contribution can be measured with special cameras [51.48, 49]: pyrheliometers with different fields of view [51.50] or RSIs [51.51]. For remote sites, RSI is the only commercially available measurement option. Camera-based instruments for circumsolar radiation measurements are only used at research stations, as they are highly maintenance intense and expensive.

Solar spectral irradiance measurements have so far been limited mainly to research sites. To change this, radiative transfer calculations can be used based on simpler measurements, such as the multifilter rotating shadowband radiometer [51.52], sun photometers, or multifilter radiometers [51.53].

In recent years, measurement stations for solar tower plants have also started including meteorological optical-range (MOR) measurements to obtain information on the beam attenuation between the mirrors and the receiver on the tower. Chapter 13 introduced visibility sensors. It is important to mention that the conversion from the MOR [51.54] to the required broadband beam attenuation is not a simple task (broadband refers to the wavelength range from about 280 to 4000 nm), as the instruments and the definition of MOR do not refer to broadband radiation. Therefore, correction functions are required [51.55].

Also, soiling rate measurements have been included in meteorological stations for solar energy applications in the last decade. For PV, such measurements can be obtained by comparing the short-circuit current or power output of cleaned and uncleaned PV reference cells or modules [51.56]. For concentrating collectors with mirrors, the reflected direct normal irradiance is compared to G_b [51.57], or reflectance measurements are carried out on exposed mirror samples.

Solar radiation measurements are important input for the accurate forecasting of solar radiation. Additional ground measurements are provided in the form of all-sky images mainly relating to forecasting for the next 15 min. Such images of the complete upper hemisphere are taken with fisheye lenses or curved mirrors. The images can be used to detect clouds and to track and forecast their position. Finally, with additional assumptions on the clear-sky atmosphere, this allows the prediction of the solar irradiance in a power plant or in an area with several power plants (e.g., a city with many PV rooftop systems). For these irradiance forecasts, the cloud height is required if spatially resolved irradiance maps are to be forecasted. Cloud height measurements can come from different sources, such as ceilometers or multiple all-sky imagers. Current research indicates that all-sky imagers are the preferable option [51.58]. All-sky imagers have also been used to measure the current downwelling shortwave irradiance (G, G_b). However, such methods do not reach the accuracy required for solar energy applications so far.

At times, PV reference cells are also applied in solar resource assessment to obtain data that are more comparable to the expected production of PV collectors. While thermopile pyranometers are designed to measure broadband irradiance with low errors introduced by the incidence angle, temperature, and spectral effects, such effects occur in PV modules and reference cells. If the applied reference cells are similar to the PV module of interest, the data collected with the reference cell can be used more easily to calculate the expected PV production, as the mentioned errors do not have to be modeled in the PV plant yield model. However, most PV models include the modeling of these errors, so that PV reference cell data must be used with great care. Furthermore, PV reference cell measurements are difficult to compare with other existing datasets from pyranometers and satellites, which further complicate their application. Therefore, measurements with reference cells are rather carried out as additional measurements next to other radiometers. A dataset that only contains PV reference cell data must currently be considered of lower quality. Advantages and disadvantages of the measurement options mentioned for solar energy applications are included in Table 51.2.

Table 51.2 Advantages and disadvantages of selected measurement devices with respect to energy meteorology

Device	Advantages	Disadvantages
Cup anemometer	Can be calibrated in wind tunnel, calibration standards exist	Needs masts for locating at height of rotor plane, extrapolation to greater heights necessary, limited turbulence measurements, horizontal wind speed only
Sonic anemometer	High-frequency wind measurements, turbulence measurements, all three wind components available	Rain droplets or ice at the sound transducers can disturb the measurements, appropriate calibration standards have not been developed
Wind lidar	Does not need calibration, direct profile measurements	Measurement obstructed by fog, clouds, and precipitation
SAR on satellites	Not obstructed by clouds, operates day and night, large areas are covered simultaneously	Several days between satellite overpasses, offshore application only, near-surface winds only

Table 51.2 (Continued)

Device	Advantages	Disadvantages
Thermopile pyranometer	Achieves the highest available accuracy for tilted irradiance measurements under well-maintained conditions in high frequency	Require frequent cleaning and other maintenance (daily). Available stations are rare, especially for long-term data sets (> 10 years). Costs
Thermopile pyrheliometer	Achieves the highest available accuracy for direct irradiance measurements under well-maintained conditions in high frequency	Requires frequent cleaning and other maintenance (daily) and expensive and error-prone solar trackers. Available stations are rare, especially for long-term datasets (> 10 years). Costs
Rotating shadowband irra-diometer	Simple, robust, frequent, and cheap option for de-termination of global horizontal, direct normal and global tilted irradiance. Only less frequent cleaning required compared to instruments with clear optics (e.g., every week)	Achieves a lower accuracy compared to thermopile sensors even if correction functions for systematic errors are applied. Available stations are rare, especially for long-term datasets (> 10 years)
PV reference cell	Measures an output signal close to that of specific corresponding PV modules in high frequency	Difficult to compare with more frequently available broadband irradiance data and incompatible with many PV plant models. Available stations are rare, especially for long-term datasets (> 10 years)
Ground-based spectrora-diometer	Accurate and frequent measurements of solar spectra can be obtained	Difficult to maintain, too expensive for most stations
Satellite-based imager for irradiance measurements	Long-term datasets (> 10 years) available for the whole planet, even spectrally resolved. No data gaps, maintenance issues. Relatively low costs, as satellites are paid by somebody else	Lower accuracy compared to ground-based methods, lower temporal frequency (15 min compared to 1 min or higher)
Camera-based circumsolar radiation measurement	Some systems can reach high accuracy. Complete information for plant models measured, including sunshape	High costs and maintenance requirements
Pyrheliometer pairs with different field of views for circumsolar radiation measurements	High accuracy for the circumsolar contribution and integrated irradiance for one angular interval	No angular resolved radiance, only integrated irra-diance for one angular interval. Modeling needed for determination of sunshapes. Daily maintenance required, error-prone to soiling
Rotating shadowband irra-diometers for circumsolar radiation measurements	Low maintenance effort, simple data evaluation	No angular resolved radiance, only integrated irradi-ance for one angular interval. Modeling needed for determination of sunshapes. Lower accuracy com-pared to camera and pyrheliometer-based methods
Beam attenuation mea-surement based on MOR measurements	Simple measurement method	Requires correction for spectral and broadband effect
Satellite-based imager for circumsolar irradiance measurements and beam attenuation measurements	Long-term datasets (> 10 years) can be determined for the whole planet. No data gaps, maintenance issues. Relatively low costs, as satellites are paid by somebody else	Still in development phase, low accuracy compared to ground measurements
Soiling-rate measurement with test mirrors or test PV cells/modules	Frequent measurements of cleanliness and soiling rate	Maintenance intense
Ground-based all-sky im-ager for forecasting	Highly temporally and spatially resolved irradiance data can be determined	Costs, maintenance. Forecasts confined to the next approximately 15 min
Satellite-based imager for forecasting of irradiance	Forecasts can be determined for the whole planet. No data gaps, maintenance issues. Relatively low costs, as satellites are paid by somebody else. Forecast horizon up to approximately 6 h	Lower accuracy, temporal and spatial resolution than all-sky imagers

51.4.5 Satellite–Based Radiation Measurements

As explained in Sect. 51.3.2, satellite-based surface radiation measurements are a standard data source for solar energy applications to create the required long-term datasets ($\approx$ 10 years or more). The applied methods and technology are explained in Chap. 40 on airborne radiation sensors and in Sect. 22.4.3 on cloud observations that are an important intermediate result. For solar energy applications the postprocessing of these data is of high importance.

As the accuracy of satellite-derived data is significantly lower than that of well-maintained ground measurements, the latter are frequently merged with the satellite data to create bankable solar resource data during the planning phase of the power plant. This is especially relevant for the planning of solar plants with several MW power output, as financing costs depend on the risk of the project and, hence, on the uncertainty of the resource data. The final long-term dataset is created by merging the at least 1 year-long dataset from ground measurements and the satellite-derived data [51.59]. Plant yield calculations for the feasibility study and plant layout are carried out with these long-term datasets. For the detailed design of the plant, also measurement data are used due to the higher temporal resolution and accuracy.

Satellite-derived irradiance data are also applied at times for the power plant monitoring of some medium-sized facilities. Furthermore, the data are key for radiation forecasts with a horizon of up to 6 h. Cloud-motion vectors are determined from series of satellite images, and the detected cloud positions are then extrapolated to the future. These predicted cloud positions are then used to calculate the solar irradiance.

Apart from broadband direct normal, global horizontal, and global tilted irradiance, satellite data may also be used to derive further parameters, such as circumsolar radiation, beam attenuation in tower plants, and spectral irradiance. For circumsolar radiation, such efforts [51.60] are still in the development phase and are not used commercially. The same holds for beam attenuation studies. Spectral irradiance can be derived from satellite data [51.61], and such datasets have already been integrated in selected PV yield analysis tools [51.62].

51.4.6 Comparison of Methods

The advantages and disadvantages of some of the mentioned measurement methods for wind (first four lines) and solar (rest of the table) energy applications are compared in Table 51.2.

51.5 Specifications

Users of wind speed measurement data for the assessment of available wind energy often request a rather high accuracy in the order of 1%, because wind energy depends on the third power of the wind speed (51.1). A 1%-error in wind speed thus means up to 3% error in wind energy. Therefore, most guidelines [51.6] favor cup anemometers as in-situ devices for wind energy purposes, because they can be carefully calibrated in wind tunnels to achieve the requested accuracy. Remote-sensing instruments cannot be calibrated in the same way as cup anemometers in wind tunnels. Actually, they do not even need to be calibrated, because they are based on fundamental physical principles. Please note, that wind data from remote sensing and in-situ measurements are not fully comparable due to the different measurement principles (cup anemometers are in-situ instruments; sodars and wind lidars are volume-averaging instruments).

Specifications of solar energy related instruments are also included in Table 51.3.

While cup anemometer data is nearly always available, wind lidar data is not available during fog and precipitation events. The vertical range of optical remote sensing can also be limited by the aerosol content of the atmosphere. Very low aerosol concentrations may lead to insufficient signal-to-noise ratios of the backscattered signal.

Table 51.3 Specifications of selected measurement methods for the application in the field of generation of renewable energies

Method	Typical total uncertainty	Temperature range (°C)	Humidity range (%)
Cup anemometer	±1% [51.6]	−10 to 50	0–100
Wind lidar	±0.1 m s^{-1} (Class A), ±0.5 m s^{-1} (Class B), ±1.0 m s^{-1} (Class C) [51.34]	−20 to 40	0–100
Thermopile pyrheliometer	0.7% (1 min resolution)	−40 to 80	0–100
Thermopile pyranometer	1.2% (1 min resolution)	−40 to 80	0–100
Silicon pyranometer with correction functions for global horizontal measurements	3.5% (1 min resolution)	−40 to 65	0–100
Twin RSI	3.5% (global horizontal and direct normal irradiance in 10 min resolution)	−40 to 65	0–100
Satellite-derived irradiance data after site adaptation with ground measurements	Annual average: 4% for global horizontal irradiance, (for complex areas higher) Hourly: 7% to 35% for global irradiance (depending on cloud, aerosol and ground conditions) Direct irradiances errors are typically about twice the errors for global horizontal irradiance [51.2]	Does not apply	Does not apply
Beam attenuation measurements with MOR sensors	$\approx$ 5% in terms of broad band transmittance over a path of 1 km [51.55]	−55 to 65	0–100
Camera-based circumsolar radiation measurements [51.49]	15% for circumsolar contribution, minimum 0.01	−10 to 45	0–100
Pyrheliometer-based circumsolar radiation measurements [51.50]	15% for circumsolar contribution, minimum 0.01	−40 to 65	0–100
RSI-based circumsolar radiation measurements	20% to 30% for circumsolar contribution, minimum 0.02 [51.51]	−40 to 65	0–100
Soiling rate measurement systems	$\approx$ 0.2%/day [51.57]	−40 to 65	0–100
Ground-based spectroradiometers	0.2 nm wavelength uncertainty below $\approx$ 1000 nm, 5% spectral irradiance (350−1600 nm)	−10 to 40	0–100
Tipping bucket (Cs700) precipitation measurement	2%	0 to 70	0–100
Optical weather sensor (FD12P) with precipitation measurement	30%	−40 to 55	0–100

51.6 Quality Control

Planning, siting, and operation of renewable energy facilities need data of high accuracy and quality, because the financial success of these facilities often crucially depends on data quality. While companies and organizations working in planning and siting of energy converters have to fulfil the usual data quality demands for their measurement devices (mostly according to the instructions given by the manufacturers of these instruments), instruments mounted at or near to operating energy facilities should be included in the data quality procedures of these installations. Please refer to the respective chapters on specific quality control procedures for the different instruments. For cup anemometers, see also [51.63], for sonic anemometers [51.64], and for wind lidars [51.34]. For solar energy applications, specific minor adaptations of the common quality checks exist; see, e.g., [51.65].

51.7 Maintenance

The demands and strategies for the maintenance of instruments delivering meteorological parameters for planning, siting, and operation of energy conversion facilities are very much similar to those given for data quality in Sect. 51.6 above. For the required maintenance procedures please refer to the respective chapters on the specific instruments. It should be mentioned again that the feasible maintenance intensity for solar resource assessment stations might be more limited than recommendations for solar radiation measurements as already discussed in Sect. 51.4.4.

51.8 Application

This section gives two application examples of measurements. The first example refers to the wind and thermal stability conditions for the operation of offshore wind parks; the second example displays radiation measurements relevant for solar power plants.

Fig. 51.3 Stability wind rose indicating the frequency (number of 10-min intervals per 12° wind direction sector) of atmospheric stability. *Lines* are labeled in terms of the stability measure z/L, where z is the height above ground, and L is the Obukhov length. *Blue* and *red shading* indicate stable and unstable stratification, respectively. The higher the value of z/L, the stronger the stability. Data are from the FINO 1 offshore platform in the North Sea for the whole year of 2005 at a height of 60 m above the sea surface. Data is available from http://fino.bsh.de/. Only data with wind speeds between the cut-in ($5\,\mathrm{m\,s^{-1}}$) and cut-off ($25\,\mathrm{m\,s^{-1}}$) wind speed were considered (after [51.41]) ▶
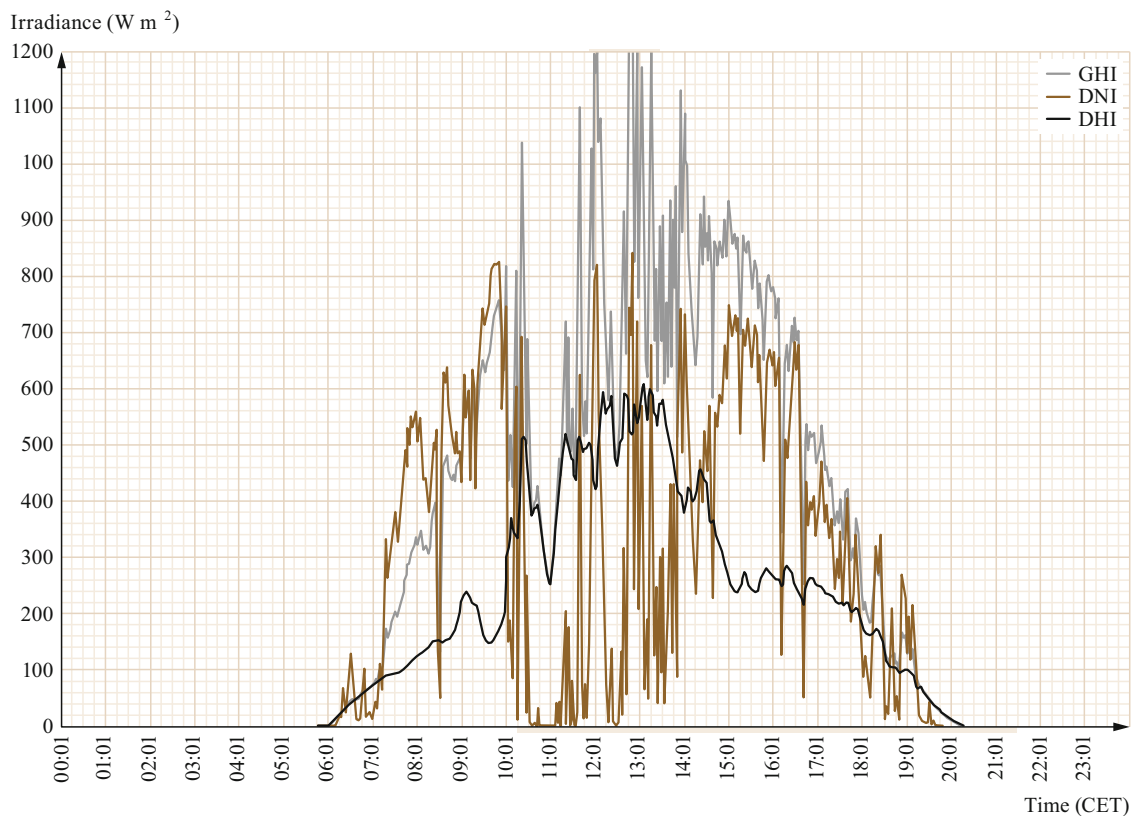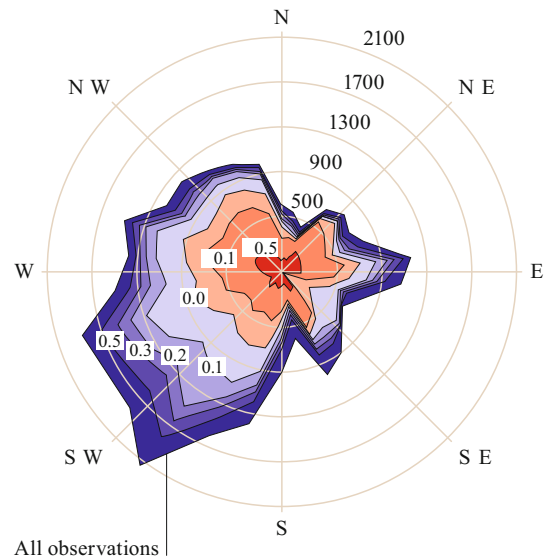
Fig. 51.4 Irradiance measurements in 1 min-resolution from a meteorological station equipped with thermopile sensors close to Tabernas, Spain on 23.05.2018 (GHI: global horizontal irradiance, DNI: direct normal irradiance, DHI: diffuse horizontal irradiance)

51.8.1 Wind Energy Applications

It has been stated in this chapter that atmospheric turbulence (at the end of Sect. 51.3.1) and wakes behind wind turbines (at the end of Sect. 51.2.1) not only depend on wind speed but also on the atmospheric thermal stability. Therefore, for the assessment of wake interactions and fatigue issues of wind turbines, both parameters have to be assessed together. Figure 51.3 gives an example of an evaluation of 10 min-mean data obtained at 60 m above sea level at the FINO1 platform in the German Bight from a cup anemometer for wind speed and from a sonic anemometer for atmospheric stability. The FINO1 platform was erected for the investigation of the wind conditions in the marine atmospheric boundary layer in the German Bight. These data serve for the planning of the large offshore wind farms, which are presently being erected there. Figure 51.3 demonstrates that wind direction and thermal stability are correlated with each other offshore [51.41]. Stable atmospheric stability mainly occurs with southwesterly wind directions. Southwest is the prevailing wind direction in warm sectors of cyclones on the Northern Hemisphere, where warmer air is advected over colder waters. Likewise, we observe unstable conditions mainly occurring with northwesterly winds. This is the prevailing wind direction in the cold air masses behind the cold front of cyclones in the Northern Hemisphere. Such a correlation is not observed for onshore conditions, because here the diurnal day–night variation of the thermal stability dominates.

51.8.2 Solar Energy Applications

As was already briefly mentioned in Sects. 51.3.2, 51.4.3, and 51.4.4, different measurement techniques have different applications. As an example the results of typical measurement stations with thermopile pyranometers and pyrheliometers for 1 day are shown in Fig. 51.4. Such graphs are used for the daily quality control of the collected measurements. Figure 51.5 shows a histogram of the three irradiance components for a measurement station in India in April 2018. Such histograms are used as a tool to evaluate the variability of the solar irradiance.
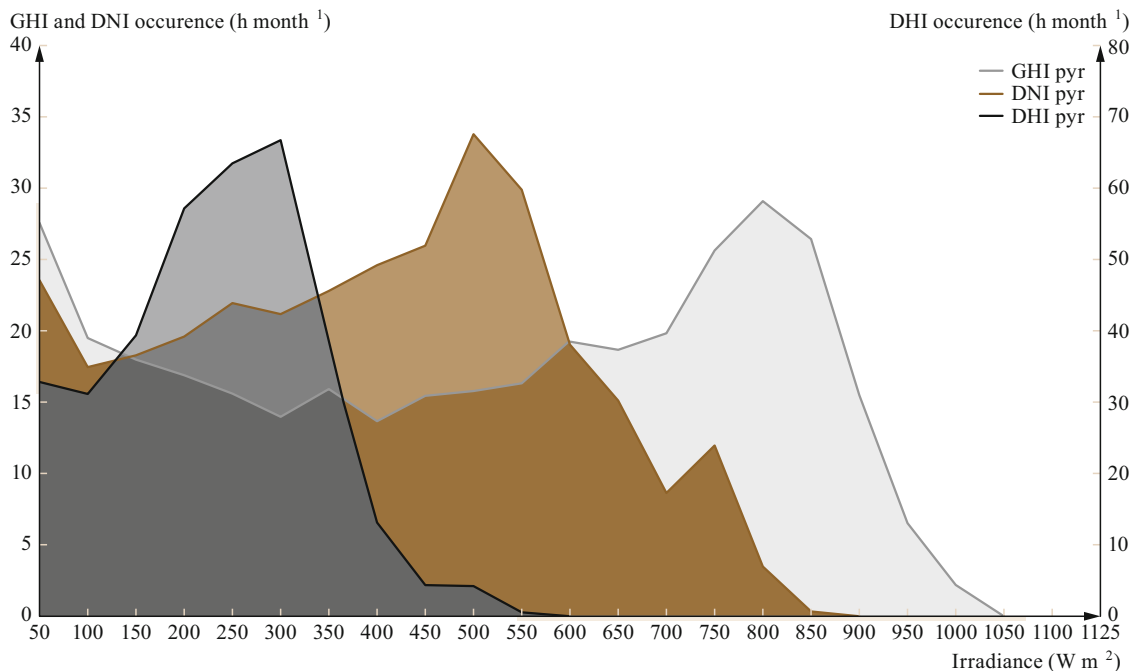
Fig. 51.5 Histogram of irradiance measurements with thermopile sensors from a meteorological station close to Greater Noida India in April 2018 derived based on data in hourly resolution (GHI pyr: global horizontal irradiance measured by a pyranometer, DNI pyr: direct normal irradiance by a pyrheliometer, DHI pyr: diffuse horizontal irradiance by a shaded pyranometer). Irradiance is given in units of $W\,m^{-2}$ within a $\pm 25\,W\,m^{-2}$ interval. Courtesy of Birk Kraas, CSPS Services, Stefan Wilbert, DLR

51.9 Future Developments

Measurement techniques for atmospheric parameters at hub height of wind turbines and over the area swept by their rotors have changed. In-situ measurements by cup and sonic anemometers are no longer fully sufficient. The growing hub heights and upper tip heights of the turbine rotors make it more and more impossible to perform in-situ measurements from masts specially erected for this purpose. Therefore, in many cases, ground-based remote sensing has replaced mast measurements in the last few years. Overviews of the basic abilities to probe the atmospheric boundary layer by ground-based remote sensing are given in [51.28, 32]; however, the development of some of the techniques has proceeded in the last 7 to 8 years since their publication. The substitution process from in-situ to remote-sensing measurements is to be accompanied by scientific investigations that compare the wind and turbulence data obtained from masts and remote-sensing techniques. Such investigations are continuing and have already led to rewritten standards for measurement procedures [51.6]. Given the present state of instrument development, optical techniques such as wind lidars will be the main measurement tools of the future [51.66]. SAR satellite image evaluation techniques are presently evaluated by data from in-situ aircraft data and may become an increasingly important tool for marine wind assessment [51.41].

However, not only wind conditions must be captured by ground-based remote sensing. It has become increasingly clear that atmospheric thermal stability is a really important parameter for the assessment of wind energy. Increasing stability (potential temperature increases with height above ground) reduces turbulence intensity, increases vertical wind shear, and prolongs wakes of wind turbines and entire wind farms. Devices for ground-based remote sensing of temperature are still limited in their capabilities. Passive radiometers (Chap. 41) have a very coarse vertical resolution (50–100 m); active devices such as Raman lidars (Chap. 25) still require large technical efforts and have a low signal-to-noise ratio in the daytime due to disturbing sunlight. RASS (Chap. 23) is not a perfect alternative, as it cannot be operated in the vicinity of settlements because of its audible acoustic signals.

With respect to solar energy, future developments will surely be related to increase the accuracy of ground and satellite-based measurements of all relevant parameters. The respective guidelines are under revision or have been revised recently [51.67]. For ground-based sensors, this will, on the one hand, be achieved by increasing their accuracy under well-maintained conditions. However, improving their robustness and simplicity and their maintenance requirements – especially including the need for frequent cleaning – is another way to improve the accuracy. Future developments will also include alternatives to thermopile sensors and the required corrections for systematic errors. For satellite-derived irradiance, accuracy improvement will be developed by applying higher temporal, spectral, and spatial resolutions. The speed of this enhancement will depend on the deployment of the next generations of satellites. Some of the mentioned parameters related to solar energy are still in early development stages (e.g., satellite-derived attenuation and circumsolar radiation measurements). Such methods should be elaborated further in the future.

51.10 Further Readings

A thorough introduction into wind energy meteorology can presently be obtained from two books:

- S. Emeis: Wind Energy Meteorology – Atmospheric Physics for Wind Power Generation, 2nd edn. (Springer, Heidelberg 2018) XXVI + 255 pp.
- L. Landberg: Meteorology for Wind Energy. Wiley, XIX+204 pp. (2016)

Related to solar energy meteorology:

- M. Sengupta, A. Habte, C. Gueymard, S. Wilbert, D. Renné, P. Blanc, A. Dobos, E. Lorenz, R. Meyer, D. Myers, L. Ramírez, K.P. Nielsen, A. Lopez, J. Kleissl, J. Remund, J.A. Ruiz-Arias, R. Perez, J. Polo, L.M. Pomares, M. Suri, T. Stoffel, F. Vignola, S. Wilcox, J. Wood, Y. Xie, L. Zarzalejo. Best Practices Handbook for the Collection and Use of Solar Resource Data for Solar Energy Applications. Second Edition, NREL Technical Report NREL/TP-5D00-68886, 238 pp. (2017)

A broad overview on all renewable energy techniques can be found in:

- M. Kaltschmitt, W. Streicher, A. Wiese: Renewable Energy (Springer, Heidelberg 2007), XXXII+564 pp. A revised 5th German edition of this book appeared in 2013.

References

51.1 S. Emeis: *Wind Energy Meteorology − Atmospheric Physics for Wind Power Generation*, Green Energy and Technology, 2nd edn. (Springer, Cham 2018)

51.2 M. Sengupta, A. Habte, C. Gueymard, S. Wilbert, D. Renné, T. Stoffel: *Best Practices Handbook for the Collection and Use of Solar Resource Data for Solar Energy Applications*, 2nd edn. (NREL, Golden 2017), NREL/TP-5D00-68886

51.3 C.S. Kaunda, C.Z. Kimambo, T.K. Nielsen: Hydropower in the context of sustainable energy supply: A review of technologies and challenges, ISRN Renew. Energy (2012), https://doi.org/10.5402/2012/730631

51.4 L. Dubus, S. Muralidharan, A. Troccoli: What does the energy industry require from meteorology? In: *Weather & Climate Services for the Energy Industry*, ed. by A. Troccoli (Palgrave Macmillan, Cham 2018)

51.5 ISO 9488: *Solar Energy Vocabulary* (ISO, Geneva 1999)

51.6 IEC 61400-12-1: *Wind Energy Generation Systems − Part 12-1: Power Performance Measurements of Electricity Producing Wind Turbines* (VDE, Berlin 2017)

51.7 A. Peña, R. Floors, A. Sathe, S.E. Gryning, R. Wagner, M.S. Courtney, X.G. Larsén, A.N. Hahmann, C.B. Hasager: Ten years of boundary-layer and wind-power meteorology at Høvsøre, Denmark, Bound.-Layer Meteorol. **158**(1), 1−26 (2016)

51.8 M. Türk, K. Grigutsch, S. Emeis: The wind profile above the sea−Investigations basing on four years of FINO 1 data, DEWI Magazin **33**, 12−16 (2008)

51.9 J. Mann, N. Angelou, J. Arnqvist, D. Callies, E. Cantero, R. Chávez Arroyo, M. Courtney, J. Cuxart, E. Dellwik, J. Gottschall, S. Ivanell, P. Kühn, G. Lea, J.C. Matos, J.M.L.M. Palma, L. Pauscher, A. Peña, J. Sanz Rodrigo, S. Söderberg, N. Vasiljevic, C. Veiga Rodrigues: Complex terrain experiments in the new European wind atlas, Philos. Trans. R. Soc. **375**(2091), 20160101 (2017)

51.10 A. Clifton, S. Schreck, G. Scott, N. Kelley, J.K. Lundquist: Turbine inflow characterization at the National Wind Technology Center, J. Sol. Energy Eng. **135**, 031017 (2013)

51.11 A.B. Mouchot: *La Chaleur Solaire et ses Applications Industrielles* (Gauthier-Villars, Paris 1869)

51.12 M.L. Wesely: Simplified techniques to study components of solar radiation under haze and clouds, J. Appl. Meteorol. **21**, 373−383 (1982)

51.13 G.O.G. Löf, J.A. Duffie, C.O. Smith: World distribution of solar radiation, Sol. Energy **10**, 27−37 (1966)

51.14 H.C.S. Thom: The rational relationship between heating degree days and temperature, Mon. Weather Rev. **82**, 1−6 (1954)

51.15 H. Landsberg: Bioclimatology of housing. In: *Recent Studies in Bioclimatology*, Meteorological Monographs, Vol. 2 (AMS, Boston 1954) pp. 81−98

51.16 A. Betz: Das Maximum der theoretisch möglichen Ausnützung des Windes durch Windmotoren, Z. Gesamte Turbinenwes. **26**, 307−309 (1920)

51.17 A. Betz: *Wind-Energie und ihre Ausnutzung durch Windmühlen* (Vandenhoeck & Ruprecht, Göttingen 1926)

51.18 W. Weibull: A statistical distribution function of wide applicability, J. Appl. Mech. **73**, 293−297 (1951)

51.19 E.J. Gumbel: *Statistics of Extremes* (Columbia Univ. Press, New York, London 1958)

51.20 R. Wagner, B. Cañadillas, A. Clifton, S. Feeney, N. Nygaard, M. Poodt, C. St. Martin, E. Tüxen, J.W. Wagenaar: Rotor equivalent wind speed for power curve measurement − Comparative exercise for IEA Wind Annex 32, J. Phys. Conf. Ser. **524**(1), 012108 (2014)

51.21 C.A. Paulson: The mathematical representation of wind speed and temperature profiles in the unstable atmospheric surface layer, J. Appl. Meteorol. **9**, 857−861 (1970)

51.22 U. Högström: Non-dimensional wind and temperature profiles in the atmospheric surface layer: A re-evaluation, Bound.-Layer Meteorol. **42**, 55−78 (1988)

51.23 J.A. Businger, J.C. Wyngaard, Y. Izumi, E.F. Bradley: Flux profile relationships in the atmospheric surface layer, J. Atmos. Sci. **28**, 181−189 (1971)

51.24 A.J. Dyer: A review of flux-profile relations, Bound.-Layer Meteorol. **7**, 363−372 (1974)

51.25 A.A.M. Holtslag, H.A.R. de Bruin: Applied modeling of the nighttime surface energy balance over land, J. Appl. Meteorol. **27**, 689−704 (1988)

51.26 M. Bartos, M. Chester, N. Johnson, B. Gorman, D. Eisenberg, I. Linkov, M. Bates: Impacts of rising air temperatures on electric transmission ampacity and peak electricity load in the United States, Environ. Res. Lett. **11**(11), 114008 (2016)

51.27 EN 50341-1:2012: *Overhead Electrical Lines Exceeding AC 1 kV. General Requirements − Common Specifications* (CENELEC, Brussels 2012)

51.28 S. Emeis: *Measurement Methods in Atmospheric Sciences − In Situ and Remote*, Quantifying the Environment, Vol. 1 (Borntraeger, Stuttgart 2010)

51.29 VDI 3786-2: *Environmental Meteorology − Meteorological Measurements − Wind* (Beuth, Berlin 2018)

51.30 VDI 3786-12: *Environmental Meteorology − Meteorological Measurements − Turbulence Measurements with Sonic Anemometers* (Beuth, Berlin 2019)

51.31 T.F. Pedersen, J.-Å. Dahlberg, A. Cuerva, F. Mouzakis, P. Busche, P. Eecen, A. Sanz-Andres, S. Franchini, S.M. Petersen: *ACCUWIND − Accurate Wind Speed Measurements in Wind Energy (Summary Report)* (Risø National Laboratory, Roskilde 2006), Risø Report Risø-R-1563(EN), http://www.windspeed.co.uk/ws/public/ACCUWIND-ris-r-1563.pdf, Accessed 21 July 2021

51.32 S. Emeis: *Surface-Based Remote Sensing of the Atmospheric Boundary Layer*, Atmospheric and Oceanographic Sciences Library, Vol. 40 (Springer, Dordrecht, Heidelberg, London, New York 2011)

51.33 VDI 3786-11: *Environmental Meteorology − Ground-Based Remote Sensing of the Wind Vector and the*

Vertical Structure of the Boundary Layer – Doppler Sodar (Beuth, Berlin 2015)

51.34 ISO 28902-2: *Air Quality – Environmental Meteorology – Part 2: Ground-Based Remote Sensing of Wind by Heterodyne Pulsed Doppler Lidar* (ISO, Geneva 2017)

51.35 VDI 3786-18: *Environmental Meteorology – Ground-Based Remote Sensing of Temperature – Radio-Acoustic Sounding Systems (RASS)* (Beuth, Berlin 2010)

51.36 J. Röttger, M.-F. Larsen: UHF/VHF radar techniques for atmospheric research and wind profiler applications. In: *Radar in Meteorology*, ed. by D. Atlas (AMS, Boston 1990) pp. 235–281

51.37 VDI 3786-17: *Environmental Meteorology – Ground-Based Remote Sensing of the Wind Vector – Wind Profiler Radar* (Beuth, Berlin 2007)

51.38 W. Koch, F. Feser: Relationship between SAR-derived wind vectors and wind at 10-m height represented by a mesoscale model, Mon. Weather Rev. **134**, 1505–1517 (2006)

51.39 M.B. Christiansen, C.B. Hasager: Wake effects of large offshore wind farms identified from satellite SAR, Remote Sens. Environ. **98**, 251–268 (2005)

51.40 C.B. Hasager, P. Vincent, R. Husson, A. Mouche, M. Badger, A. Peña, P. Volker, J. Badger, A. Di Bella, A. Palomares, E. Cantero, P.M.F. Correia: Comparing satellite SAR and wind farm wake models, J. Phys. Conf. Ser. **625**, 012035 (2015)

51.41 A. Platis, S.K. Siedersleben, J. Bange, A. Lampert, K. Bärfuss, R. Hankers, B. Canadillas, R. Foreman, J. Schulz-Stellenfleth, B. Djath, T. Neumann, S. Emeis: First in situ evidence of wakes in the far field behind offshore wind farms, Sci. Rep. **8**, 2163 (2018)

51.42 ISO 9901: *Solar Energy – Field Pyranometers – Recommended Practice for Use* (ISO, Geneva 1990)

51.43 WMO: *Guide to Instruments and Methods of Observation*, WMO-No. 8, Volume I – Measurement of Meteorological Variables (World Meteorological Organization, Geneva 2018)

51.44 L.J.B. McArthur: *Baseline Surface Radiation Network (BSRN). Operations Manual (Version 2.1)* (WMO, Geneva 2005), WCRP-121, WMO/TD-No. 1274

51.45 S. Wilbert, S. Kleindiek, B. Nouri, N. Geuder, A. Habte, M. Schwandt, F. Vignola: Uncertainty of rotating shadowband irradiometers and Si-pyranometers including the spectral irradiance error, AIP Conf. Proc. **1734**, 150009 (2016)

51.46 D. Schüler, S. Wilbert, N. Geuder, R. Affolter, F. Wolfertstetter, C. Prahl, M. Röger, M. Schroedter-Homscheidt, G. Abdellatif, A. Allah Guizani, M. Balghouthi, A. Khalil, A. Mezrhab, A. Al-Salaymeh, N. Yassaa, F. Chellali, D. Draou, P. Blanc, J. Dubranna, O.M.K. Sabry: The enerMENA meteorological network – Solar radiation measurements in the MENA region, AIP Conf. Proc. **1734**, 150008 (2016)

51.47 J. Badosa, J. Wood, P. Blanc, C.N. Long, L. Vuilleumier, D. Demengel, M. Haeffelin: Solar irradiances measured using SPN1 radiometers: Uncertainties and clues for development, Atmos. Meas. Tech. **7**(12), 4267–4283 (2014)

51.48 S. Schrott, T. Schmidt, T. Hornung, P. Nitz: Scientific system for high-resolution measurement of the circumsolar radiation, AIP Conf. Proc. **1616**, 88–91 (2014)

51.49 S. Wilbert, B. Reinhardt, J. DeVore, M. Röger, R. Pitz-Paal, C. Gueymard, R. Buras: Measurement of solar radiance profiles with the Sun and aureole measurement system, J. Sol. Energy Eng. **135**, 041002 (2013)

51.50 S. Wilbert, R. Pitz-Paal, J. Jaus: Comparison of measurement techniques for the determination of circumsolar irradiance, AIP Conf. Proc. **1556**, 162–167 (2013)

51.51 S. Wilbert, M. Röger, J. Csambor, M. Breitbach, F. Klinger, B. Nouri, N. Hanrieder, F. Wolfertstetter, D. Schüler, S. Shaswattam, N. Goswami, S. Kumar, A. Ghennioui, R. Affolter, N. Geuder, B. Kraas: Sunshape measurements with conventional rotating shadowband irradiometers, AIP Conf. Proc. **2033**, 190016 (2018)

51.52 L. Harrison, J. Michalsky, J. Berndt: Automated multifilter rotating shadow-band radiometer: An instrument for optical depth and radiation measurements, Appl. Opt. **33**, 5118–5125 (1994)

51.53 V. Tatsiankou, K. Hinzer, H. Schriemer, S. Kazadzis, N. Kouremeti, J. Gröbner, R. Beal: Extensive validation of solar spectral irradiance meters at the World Radiation Center, Sol. Energy **166**, 80–89 (2018)

51.54 ISO 28902-1:2012: *Air Quality – Environmental Meteorology – Part 1: Ground-Based Remote Sensing of Visual Range by Lidar* (ISO, Geneva 2012)

51.55 N. Hanrieder, S. Wilbert, R. Pitz-Paal, C. Emde, J. Gasteiger, B. Mayer, J. Polo: Atmospheric extinction in solar tower plants: Absorption and broadband correction for MOR measurements, Atmos. Meas. Tech. **8**, 3467–3480 (2015)

51.56 T. Sarver, A. Al-Qaraghuli, L.L. Kazmerski: A comprehensive review of the impact of dust on the use of solar energy: History, investigations, results, literature, and mitigation approaches, Renew. Sustain. Energy Rev. **22**, 698–733 (2013)

51.57 F. Wolfertstetter, K. Pottler, N. Geuder, R. Affolter, A.A. Merrouni, A. Mezrhab, R. Pitz-Paal: Monitoring of mirror and sensor soiling with TraCS for improved quality of ground based irradiance measurements, Energy Procedia **49**, 2422–2432 (2014)

51.58 P. Kuhn, M. Wirtz, N. Killius, S. Wilbert, J.L. Bosch, N. Hanrieder, B. Nouri, J. Kleissl, L. Ramirez, M. Schroedter-Homscheidt, D. Heinemann, A. Kazantzidis, P. Blanc, R. Pitz-Paal: Benchmarking three low-cost, low-maintenance cloud height measurement systems and ECMWF cloud heights against a ceilometer, Sol. Energy **168**, 140–152 (2018)

51.59 J. Polo, S. Wilbert, J.A. Ruiz-Arias, R. Meyer, C. Gueymard, M. Suri, L. Martin, T. Mieslinger, P. Blanc, I. Grant, J. Boland, P. Ineichen, J. Remund, R. Escobar, A. Troccoli, M. Sengupta, K.P. Nielsen, D. Renne, N. Geuder, T. Cebecauer: Preliminary survey on site-adaption techniques for satellite-derived and reanalysis solar radiation datasets, Sol. Energy **132**, 25–37 (2016)

51.60 B. Reinhardt, R. Buras, L. Bugliaro, S. Wilbert, B. Mayer: Determination of circumsolar radiation from Meteosat Second Generation, Atmos. Meas. Tech. **7**, 823–838 (2014)

51.61 R. Mueller, T. Behrendt, A. Hammer, A. Kemper: A new algorithm for the satellite-based retrieval of solar surface irradiance in spectral bands, Remote Sens. Environ. **4**, 622–647 (2012)

51.62 T. Huld, A.G. Amillo: Estimating PV module performance over large geographical regions: The role of irradiance, air temperature, wind speed and solar spectrum, Energies **8**, 5159–5181 (2015)

51.63 ISO 17713-1: *Meteorology – Wind Measurements – Part 1: Wind Tunnel Test Methods for Rotating Anemometer Performance* (ISO, Geneva 2007)

51.64 ISO 16622: *Meteorology – Sonic Anemometers/Thermometers – Acceptance Test Methods for Mean Wind Measurements* (ISO, Geneva 2003)

51.65 N. Geuder, F. Wolfertstetter, S. Wilbert, D. Schüler, R. Affolter, B. Kraas, E. Lüpfert, B. Espinar: Screening and flagging of solar irradiation and ancillary meteorological data, Energy Procedia **69**, 1989–1998 (2015)

51.66 J.-J. Trujillo, F. Bingöl, G.C. Larsen, J. Mann, M. Kühn: Light detection and ranging measurements of wake dynamics. Part II: Two-dimensional scanning, Wind Energy **14**, 61–75 (2011)

51.67 ISO 9060:2018: *Solar Energy – Specification and Classification of Instruments for Measuring Hemispherical Solar and Direct Solar Radiation* (ISO, Geneva 2018)

Stefan Emeis

Institute of Meteorology and Climate Research
Karlsruhe Institute of Technology (KIT)
Garmisch-Partenkirchen, Germany
stefan.emeis@kit.edu

Stefan Emeis is an unsalaried Professor of Meteorology at the University of Cologne, group leader at KIT, and editor-in-chief of *Meteorologische Zeitschrift*. His research mainly involves ground-based remote sensing of the atmospheric boundary layer. He has written books on measurement techniques and wind energy, organized conferences (e.g., ISARS 13, METTOOLS VI), and was awarded the Honorary Medal of the VDI and the Reinhard Süring Medal from the German Meteorological Society.

Stefan Wilbert

Institut für Solarforschung
Deutsches Zentrum für Luft- und Raumfahrt e. V. (DLR)
Almeria, Spain
stefan.wilbert@dlr.de

Stefan Wilbert works in the Institute of Solar Research at DLR in the permanent delegation at the Plataforma Solar de Almería, Spain since 2006. He is leader of the research group "Solar Energy Meteorology". Both his Diploma thesis in physics at the University of Bonn and his PhD thesis at the University of Aachen were related to meteorological effects on solar power plants. His research interests are meteorological measurements for solar energy applications, radiative transfer modelling, nowcasting of solar radiation and solar power plant simulation.

Repository KITopen

Dies ist ein Postprint/begutachtetes Manuskript.

Empfohlene Zitierung:

Zitierung der Originalveröffentlichung: